Vol.2, No.5, Page 440- 452, 2024 https://doi.org/10.59628/jast.v2i5.1054 ISSN 2958-9568 JAST

SUN PUBLISHER

مجلة جامعة صنعاء للعلوم التطبيقية والتكنولوجيا

Sana'a University Journal of Applied Sciences and Technology

https://journals.su.edu.ye/index.php/jast/

Line-of-Sight Probability Models for 5G/6G Millimeter-Wave Networks: A Review

Basheer Ameen Raddwan [1] * **and Ibrahim Ahmed Al-Baltah** [1,2]

[1] **Department of Information Technology, Faculty of Computer Science and IT, University of Sana'a, Sana'a, Yemen,**
[2] **Department of Information Technology, Faculty of Science and Engineering, Al-Hikma University, Sana'a, Yemen**

*Corresponding author: basheer@su.edu.ye

Abstract

In the fifth-generation (5G) and future wireless networks, coverage planning for millimeter-wave (mm-wave) networks in a three-dimensional (3D) urban environment depends on the communication channel and line-of-sight (LoS) probability models. This is especially true when there are big stationary obstructions. The current literature lacks a complete review of the existing LoS probability models. To bridge this gap, this paper reviews modeling approaches and mathematical models of the LoS probability. We discovered that, due to the complexity of modeling a large number of 3D layouts, most existing models have focused on a few urban layouts. We developed a 3D synthetic urban layout generator that is based on game engine technology to simulate any ITU-R P.1410 urban layouts and collect the ray-tracing. We provided a proof-of-concept to show that the game technology could handle the complexity of simulating ray-tracing in 3D urban environments. Moreover, we addressed some of the biggest challenges and gaps in the current LoS probability literature and suggested some valid opportunities.

Article Info

Keywords:
Line-of-sight probability model, ray-tracing, air-to-ground communication channels, unmanned aerial vehicles, ground-to-ground, air-to-air, large static blockages, urban

Article History:
Received: 10-June-2024,
Revised: 10-July-2024,
Accepted: 22-September-2024,
Available online: 31 October 2024.

1. INTRODUCTION

In the recent past, there has been an increasing amount of interest in studying air-to-ground (A2G) or ground-to-air (G2A) communications. The emergence of unmanned aerial vehicles (UAVs), recognized for their cost and maneuverability in operation, is primarily responsible for this. While UAVs in the fifth generation (5G) networks and beyond are capable of serving as wireless network users, they can also function as base stations or relays to enhance coverage in hotspots or areas affected by natural disasters. Furthermore, cellular network operators may utilize high frequencies, specifically millimeter waves (mm-wave), to achieve higher data throughput [1], [2], [3].

The existence of barriers that obstruct the signal between the transmitter and receiver has a major impact on mm-waves. The distance between objects also results in rapid signal attenuation. For example, the mm-wave band is attenuated by 15–25 dB when blocked by the human body [4], [5].

Consequently, investigating the feasibility of a direct line-of-sight (LoS) between the UAVs and the ground user terminals (gUTs) has emerged as a significant research topic. The LoS probability is a critical part of the communication channel models, regardless of the communication link direction. The LoS concept describes a situation where it is possible to connect a straight line between the UAV and the gUT without any blocker in the middle, as illustrated in figure 1.

Despite the existence of numerous LoS probability models, the current literature lacks a comprehensive review or performance evaluation to support future research that relies on accurate three-dimensional channel models. For example, planning millimeter-wave (mm-wave) networks relies on the communication channel's decent accuracy to guarantee the target throughput. Nevertheless, network designers rely on throughput estimation to decide where to deploy edge computing data centers to support data offloading services. These and other examples underscore the importance of assessing the current LoS probability models in standard urban

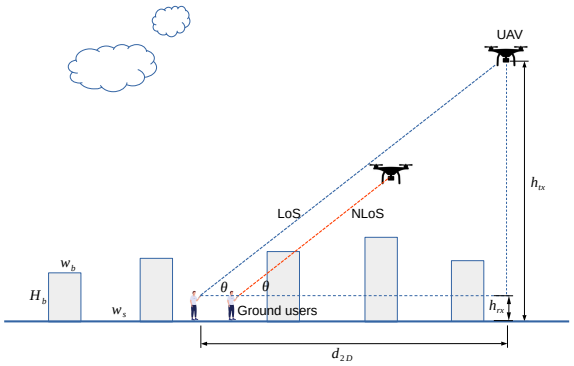

Figure 1. Communication link between UAVs and outdoor ground users.

environments.

However, few recent literature reviews have discussed different aspects of modern networks, particularly the LoS probability topic. For example, [1] reviewed the future direction of using UAC-assisted cellular communications, while [3] studied the impact of adopting artificial intelligence (AI)-based methods to optimize UAV-assisted networks for internet-of-things (IoT) applications. Similar efforts to this review are presented in [6] and [7]. [6] reviewed the mathematical models that were used in assessing performance reliability for the 5G/6G mm-wave and terahertz cellular systems, whereas [7] reviewed mathematical models and methods for multi-casting in 5G mm-wave networks.

Moreover, this paper examines more LoS probability models and provides a detailed illustration of conversion methods between frequently used models. We provide detailed illustrations of various modeling approaches, mathematical models for the urban environment, distribution processes, and mathematical models of LoS probability. We found that few works simulate real-world datasets that are limited to specific urban layouts. To overcome this limitation in the empirical approach to LoS probability modeling, we developed a 3D synthetic urban layout generator that is capable of generating any 3D urban layout and, besides, can simulate ray-tracing. We leveraged the capabilities of game engine technology to generate synthetic urban layouts and simulate ray-tracing. This review provides a proof-of-concept for the game engine-based simulation that we used to produce the ray-tracing LoS in the four standard environments. We validate some recent LoS probability models by comparing them to the ray-tracing LoS.

1.1. Key contributions

The primary contributions made by this paper are:

- **Review the modeling approaches**: We present a step-by-step modeling approach to the LOS probability modeling process, including various aspects, such as the stochastic geometry of the urban layout, the urban configuration as introduced in the ITU-R P.1410-5, buildings, streets, and frequency. In this review, we collected almost everything a researcher needs to know about LoS probability modeling.
- **Review the mathematical form of LoS probability models**: We review and summarize the LoS probability models and their use cases. We compare models based on several criteria, such as the modeling approach, the communication channels, the building distributions, the'input, the compatibility with the ITU-R P.1410-5, and the generality of the model.
- **Game engine-based simulation**: The ray-tracing simulation in (3D) urban layouts is a complex task, while empirical data gathering from the real world has a high cost. Thus, we suggest exploiting the game engine's capabilities to generate 3D synthetic urban environments and simulate ray-tracing. Section 4 provides a proof-of-concept of our suggested use of game engine-based simulation in 3D urban environments. Since existing LoS probability models usually used paid simulation tools above the complexity of ray-tracing in 3D urban environments, we contributed our game engine-based simulation code to the research community, and the code is available on GitHub [8].
- **Evaluate the most recent and some LoS probability models for the A2G communication channel**: Evaluating existing LoS probability models is complementary work to this review. It validates those models on synthetic urban layouts that are similar to real-world environments. We select the most recent LoS probability models that are compatible with the ITU-R P-1410-5 urban layout to be implemented. We tested those models on four standard urban environments and analyzed their performance. The results show some limitations that can be future research opportunities.
- **Challenges and opportunities**: Based on the review and empirical evaluation of some models, we introduced some important challenges and research opportunities to enhance the LoS probability modeling and related aspects.

The modeling approaches are reviewed in Section 2. Section 3 discuss the LoS probability models. Empirical evaluation of some selected models is presented on Section 4. Section 5 discusses challenges and open opportunities. Finally, the conclusion in Section 7.

2. THE MODELING APPROACH

This section reviews the modeling approaches that are introduced in current LoS probability models. We highlight different aspects of urban layout modeling, including building distribution, heights, and widths of streets and

Table 1. Researchers have presented mathematical models of LoS probability.

Reference	Description	Reviewed LoS models	Model evaluation
[6]	Looked at the mathematical models that used in assessing performance reliability for the 5G/6G mm-wave and terahertz cellular systems	8	×
[7]	Looked at mathematical models and methods for multi-casting in 5G mm-wave networks.	9	×
This review	This article reviews LoS probability modeling methods for G2G, G2A, A2G, and A2A communication channels, with a focus on large static objects and mobility. We also conducted an experimental evaluation of LoS probability models that are compatible with ITU-R urban configuration parameters.	23	✓

buildings. We also presented the required mathematical equations to covert data from real-world datasets into suitable ray-tracing simulations.

2.1. Urban Layout

The current literature derives the LoS probability model from environmental assumptions that describe the distributions of building location and height between the transmitter and the receiver. We can categorize these assumptions into one-, two-, or three-dimensional modeling approaches. According to these categories, the LoS condition is calculated based on building heights and location distribution functions.

The simple layout is the one-dimensional distribution of buildings along the ground distance between the transmitter and the receiver. In this layout, the buildings can be processed with evenly spaced building centers, as in [9], [10], [11], and [12]. The one-dimensional Poisson process point (PPP) is introduced in [13], [14], and [15]. Inhomogeneous PPP is proposed in [16], while homogeneous PPP is presented in [17] and [18].

The two-dimensional urban layout was modeled in three scenarios, namely grid, 2D-PPP, and MPLP. The grid process involves two dimensions of evenly spaced centers of buildings and was introduced in [19], [20], [21], [22]. The 2D-PPP generates a PPP in 2D space and was introduced in [23], [24], [25], and [26]. The Manhattan Poisson Line Process (MPLP) is an urban grid deployment of buildings where the locations of streets and buildings are modeled as a pair of independent one-dimensional PPP [27], [28]. The MPLP is composed of two one-dimensional homogeneous PPPs, one in the direction of the x-axis and the other in the direction of the y-axis [29]. However, a two-dimensional uniform distribution of building positions is proposed in [30] and [31].

2.2. ITU-R Urban Configuration Model

Moreover, real-world datasets, such as City of Melbourne Open Data [32] and New York City Open Data [33], are used in the LoS probability modeling. Even though some references, such as [20], [21], and [26], depict real-world datasets that provide the position and height of buildings that are required for ray-tracing simulation, this modeling approach is still specified and cannot be generalized. The International Telecommunication Union Radio-communication Sector (ITU-R) [9] presents three statistical parameters that provide a well-known classification and description method for different types of environments. The ITU-R parameters are denoted by α, β, and γ, which can be obtained from any urban map or dataset to describe real cities or can be iterated to generate virtual cities with specific characteristics. This model has the significant advantage of being able to represent the metropolis without requiring precise knowledge of building shapes and distribution.

ITU-R defined the parameters in terms of one square kilometer as: (1) α is the ratio of land area covered by buildings to the total selected area in square kilometers. (2) β [buildings/km^2] represents the density of buildings in a unit area, which is the number of buildings in the total selected area in square kilometers. In special cases where two propagation environments have the same ratio of α, it is easy to distinguish between them with the parameter β. (3) The parameter γ describes the most probable height of buildings, which follows the Rayleigh distribution. ITU-R defines the ranges of α from 0.1 to 0.8 and β from 750 to 100 in order to describe the urban layout of buildings for suburban to dense high-rise urban environments. Whereas the ITU-R does not state the range of γ, some studies, such as [13], define the range of γ from 8 to 50 [meters] for suburban to dense high-rise urban environments.

Table 2. Four standard ITU-R P.1410 urban layout configurations [13].

Environment	α	β	γ
High-rise Urban	0.5	300	50
Dense Urban	0.5	300	20
Urban	0.3	500	15
Suburban	0.1	750	8

To facilitate the study of different communication networks, models, and/or applications, four urban scenarios were selected in the current literature [10], [34] to describe urban environments: (1) Suburban, which represents rural areas; (2) Urban, which commonly represents European cities; (3) Dense Urban, which represents

densely populated cities with buildings arranged horizontally; and (4) High-rise Urban, which represents modern cities with skyscraper-style buildings. Table 2 shows the most frequently used urban configurations.

That is, to estimate the built-up ratio from the map of a given city, calculate the ratio of the building footprint area, which we denoted by A_{bds} [km^2], to the total area of a selected region, which we denoted by A_t [km^2]. Then the built-up ratio α is expressed in Eq (1).

$$\alpha = \frac{A_{bds}}{A_t}. \tag{1}$$

In addition, the number of buildings in a square kilometer β can be determined from a given map by simply counting the building's footprints in a unit area.

2.3. Number of Buildings

The environmental setup's one-dimensional (1D)-evenly placed buildings scenario assumes that the buildings are a series of points along the ground projection of the ray between transmitter and receiver. The 1D expression implies that the building widths are null. This scenario is considered in [9], [12]. One advantage of the 1D-evenly spaced point is the ease of calculating the expected number of buildings along the line between the transmitter and the receiver. For example, the expected number of buildings n_b passed by a ray of length one kilometer equals $\lfloor\sqrt{\alpha\,\beta}\rfloor$, where $\lfloor\cdot\rfloor$ is the floor function. For a horizontal distance d_{2D} between a transmitter and a receiver, the number of buildings is denoted as $n_b = \lfloor d_{2D}\sqrt{\alpha\,\beta}\rfloor$.

We do not agree with this calculation that was presented in the literature because the total number of buildings in the square kilometer is supposed to be β, not $\alpha\beta$. Therefore, we correct the number of buildings in a square kilometer as expressed in Eq (2)

$$n_b = \lfloor d_{2D}\sqrt{\beta}\rfloor, \tag{2}$$

where d_{2D} is the ground distance between the transmitter and the receiver in kilometers. Consequently, the separation distance between buildings $\delta = d_{2D}/n_b$ and the building positions are given as a sequence of distances from the transmitter, as in Eq (3).

$$d_i = (i+0.5)\delta,\ i \in \{0,1,...,(n_b-1)\}. \tag{3}$$

2.4. Shape of Buildings

Table 2 shows that β decreases with the increase of α, indicating that building size becomes larger since there is a relationship $\alpha = \frac{\beta\mathbb{E}(w_i)\mathbb{E}(l_i)}{10^6}$, where $\mathbb{E}(w_i)$ [meters] and $\mathbb{E}(l_i)$ [meters] are the expected length and width of the i-th building, respectively. Though rectangle footprints of buildings are used in [18], [25], and a circle footprint is used in [26], the square footprint is the most commonly used in current literature. The length and width of the building can be a function that is modeled from a real with an expected length $l_b = \mathbb{E}(L_b)$ and width $w_b = \mathbb{E}(W_b)$, as expressed in [23] where L_b and W_b are the buildings' length and width random variables. The width of a square building is denoted as w_b [meter], which is modeled in Eq (4) and the resulting width of the nearby streets is expressed in Eq (5) [24], [22].

$$w_b = 1000\sqrt{\alpha/\beta}. \tag{4}$$

$$w_s = \frac{1000}{\sqrt{\beta}} - w_b. \tag{5}$$

2.5. Height of Buildings

Undoubtedly the height of buildings play the main rule in the LoS probability model, it is assumed to be a random variable, which is denoted by H_b, with a probability density function (PDF) $f_{H_b}(\cdot)$ or simply $f(\cdot)$. The Rayleigh distribution function is mainly used, however, the log-normal and the uniform distributions are also used to model the height of buildings. In [25] a uniform distribution between 10 meters and 100 meters is used while [35] distributes the building's heights with mean 30 meters and 10 meters standard deviation.

The Rayleigh distribution function is a single variable function, which is γ that also known as the mode of the scale parameter of the Rayleigh distribution. Assume that the height of the ray connecting between the transmitter and the receiver at the location of the i-th building is denoted by h_i. The probability $P[H_{b,i} \leq h_i]$ that the height of i-th building $H_{b,i}$ is less or equal the height of h_i is given by the cumulative distribution function (CDF) of the PDF function which is expressed in Eq (6).

$$F(H_{b,i} \leq h_i) = F(h_i) = \int_0^{h_i} f(x)dx. \tag{6}$$

For example, given that the Rayleigh PDF function is expressed in Eq (7).

$$f(x,\gamma) = \frac{x}{\gamma^2}\,exp\left(-\frac{x^2}{2\gamma^2}\right), \tag{7}$$

From the geometry in figure 2,

$$\frac{h_{tx}-h_{rx}}{d_{2D}} = \frac{h_i}{d_{2D}-d_i} = \frac{h_{tx}-h_i}{d_i} = \tan(\theta), \tag{8}$$

the h_i can be expressed as in Eq (9)

$$h_i = h_{tx} - \frac{d_i(h_{tx}-h_{rx})}{d_{2D}}, \tag{9}$$

where d_i is the distance from the transmitter to the i-th building. The study in [30] considers the first-order Fresnel zone and modeled the height of the LoS link at the i-th building as in Eq (10)

$$h_i = h_{tx} - \frac{d_i(h_{tx}-h_{rx})}{d_{2d}} - \frac{r_i}{cos\theta}, \tag{10}$$

where r_i is the radius of the Fresnel ellipse at the distance of building i. In [26],the probability that the height of a building is less than the LoS height, in equation (11) is

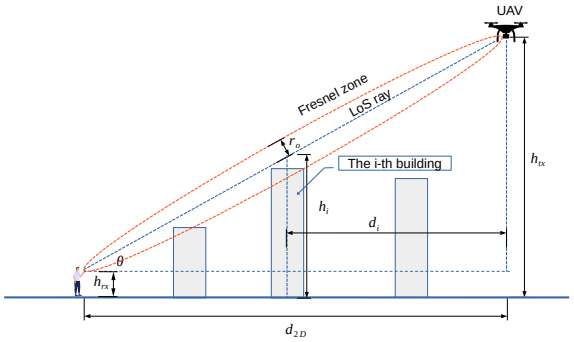

Figure 2. Geometry representation of the LoS height h_i at the i-th building for the communication link between UAVs and outdoor ground users.

modeled as a function of a distance variable between the transmitter and the receiver, denoted by d

$$h_i = \frac{d(h_{tx} - h_{rx})}{d_{2D}} + h_{rx} \tag{11}$$

Therefore, the probability of having LoS condition at the i-th building can be determine by (12).

$$F(h_i, \gamma) = \int_0^{h_i} f(x, \gamma) dx = 1 - \exp(-\frac{h_i^2}{2\gamma^2}). \tag{12}$$

Similarly, the CDF of the log-normal distribution is expressed in Eq (13).

$$F(h_i, \mu, \sigma) = \frac{1}{2}\left[1 + \exp\left(-\frac{(\ln h_i - \mu)^2}{2\sigma^2}\right)\right] \tag{13}$$

where μ and σ are the mean and the standard deviation parameters of the log-normal distribution. Both parameters can be calculated from the mean and the standard deviation of building's heights of a given dataset. The study [26] modeled these two parameters as in Eq (14) and Eq (15).

$$\mu = \ln\left(\frac{m_0}{\sqrt{1 + \frac{v_0}{m_0^2}}}\right) \tag{14}$$

$$\sigma^2 = \ln\left(1 + \frac{v_0}{m_0^2}\right) \tag{15}$$

where m_0 and v_0 are the mean and standard deviation of buildings' heights.

To determine the Rayleigh mode parameter from real-world, it is possible to follow the equation (16) that introduced in [20]. It is also possible to get the m_0 and v_0 from the Rayleigh mode parameter from the properties of the Rayleigh distribution as in equations (17) and (18).

$$\gamma = \sqrt{\frac{1}{2n_b}\sum_{i=1}^{n_b} h_i^2} \tag{16}$$

$$\mathbb{E}(H_b) = \sqrt{\frac{\pi}{2}}\gamma \tag{17}$$

$$\sigma = \sqrt{\frac{4 - \pi}{2}} \cdot \gamma \tag{18}$$

3. LINE-OF-SIGHT PROBABILITY MODELS

There are numerous ways to model the LoS probability, depending on the urban environment's layout. Existing studies present two main approaches: stochastic geometry and statistical-based methods. The geometry-based approach assumes the spatial distribution of buildings, then derives the model from the geometry of the environment's layout. This is usually suitable for 1D evenly spaced grid, MPLP, or HPPP distribution of buildings. The statistical-based approach is derived from real-world measurements. In this section, we review the existing LoS probability models to demonstrate differences, compatibility with the ITU-R model, and generality of the models. The model is considered compatible with ITU-R when it predicts the LoS status by calculating the model's variables with ITU-R configuration parameters.

The generality of the model is evaluated by the following criteria: (1) The model is composed of the building process point and height configuration parameters, which are essential to predicting different types of urban layouts. Not only α, β, and γ configuration parameters are considered, but also indirect parameters such as building and street widths, or any parameter that is derived from the main three parameters. (2) The model needs to be tested with at least two variables, such as ground distance or the height difference between the transmitter and receiver. The models that are dependent on elevation angle θ can cause confusion because one angle can represent many height-to-distance ratios, which could reduce the accuracy of the prediction. (3) The experimental validation of the model needs to be tested with different configurations, such as those in Table 2.

As in the previous section, we have categorized the existing LoS probability model according to the number of building distribution dimensions included in the modeling approach. First, we start with one-dimensional models and the ITU-R [9] that provides a standard line-of-sight probability model that applies the ITU-R urban configuration to determine the number of buildings that are likely to be located between the transmitter and the receiver to device the LoS model as a product of having the i-th building's height less than the LoS ray height at the building position. Width-less buildings are considered, while the LoS probability is calculated with the Rayleigh probability distributed function. The studies in [36], [38], and [39] are similar standard efforts that model the LoS probability for cellular network scoping the macro- and micro-cells for urban environments. These studies focus on the short-distance type of LoS probability modeling for terrestrial communication, which can be described as ground-to-ground (G2G) communication channels.

Table 3. Summary of the LoS probability models.

Reference	Approach	Channel	Building location	Building height	Model Variables	Abstract form of the LoS probability model (P_{LoS})	ITU-R	Generality
[9]	S	G2G	1D even	Ryl	(d_{2D}, h)	$\prod_{i=0}^{n_b-1}(1-\exp(-\frac{h_i^2}{a}))$	✓	✓
[10]	S	A2G	1D even	Ryl	(θ)	$a-\frac{a-b}{1+(\frac{\theta-c}{d})^e}$	x	x
[13]	G	A2G	1D-PPP	Ryl	(θ)	$\frac{1}{1+\exp(-a(\theta-b))}$	✓	x
[23]	G	G2G	2D-PPP	-	(d_{2D})	$\exp(-(ad_{2D}+b))$	x	x
[36]	S	G2G	1D even	Ryl	(d_{2D})	$\left[min(\frac{d_{Bp}}{d_{3D}},1)[1-\exp(-\frac{d_{3D}}{a})]+\exp(-\frac{d_{3D}}{a})\right]^2$	x	x
[17]	G	G2G	H-PPP	Ryl	(d_{2D})	$\exp(-\lambda min(\frac{h_b}{h_{tx}},1)d_{2D})$	x	x
[25]	G	G2G	2D H-PPP	$\mathcal{U}$	(f_c)	$\exp(-a(b\frac{d_{2D}}{h_{tx}}+c))$	x	x
[24]	S	A2A	2D-PPP	Ryl	(h_{rx}, θ)	$\exp(-a\,Q(\frac{h_{rx}}{\gamma})\cot(\theta))$	✓	x
[16]	S	A2G	1D-IPPP	Ryl	(d_{2D}, h)	$\exp\left(-a\frac{d_{2D}}{(h_{tx}-h_{rx})}erf(\frac{(h_{tx}-h_{rx})}{\sqrt{2}\gamma})\right)$	✓	✓
[26]	G	A2G	2D-PPP	Ryl	(d_{2D}, h)	$\exp\left(-a(d_{2D}-b)G((h_{tx}-h_{rx}))\right)$	x	✓
[18]	G	G2G	H-PPP	Ryl	(f_c)	$(1-\eta)^a(1-\zeta)^b$	x	x
[29]	G	G2A	MPLP	Ryl	(d_{2D})	$(1-\exp(a))\exp\left(\frac{c\cdot\exp(d)(erf(e1)-erf(e2))}{b}+\frac{c1\cdot\exp(d)(erf(e3)-erf(e4))}{b}\right)$	x	x
[11]	G	S2G	1D even	Ryl	(θ)	$\exp(-a\cdot cot(\theta))$	x	x
[12]	G	A2G	1D even	Ryl	(d_{2D})	$1-\exp(-a(\frac{h_{tx}-h_{rx}}{d_{2D}})^b)$	x	x
[19]	G	A2G	Grid	Ryl	(d_{2D}, h)	Based on [9] and Machine learning model using BPNN	✓	x
[14]	E	A2G	1D-PPP	Ryl	(h)	Machine learning using KNN and BPNN based on [36]	x	x
[20]	S	A2G	Grid	Ryl	(θ)	$a\cdot\exp(b\cdot\theta)+c\cdot\exp(d\cdot\theta)$ where $(0\leq\theta\leq 70^\circ)$	x	x
[35]	IG	G2A	$\mathcal{U}$	$\mathcal{U}$	-	$(1-a)^{b(1+c)}$	x	x
[30]	G	A2G	$\mathcal{U}$	Ryl	(θ)	$\prod_{i=1}^{n_b}\left[1-\exp(-\frac{a^2}{b})\right]$	✓	✓
[21]	S	A2G	Grid	Ryl	(θ)	$\frac{a}{1+\exp(b-c\cdot\theta)}$	✓	x
[22]	S	A2G	Grid	Ryl	(d_{2D}, h)	$1-a\cdot\exp(-b)\,(erf(c)-erf(d))$	✓	x
[31]	G	A2G	Grid	Ryl	(θ, w_b, w_s)	$1-a(erf(b1)-erf(b2))$ and algorithm	✓	x
[37]	E	S2G	-	-	(θ, ϕ)	$\exp(-a\cot(\theta))\,[bcos(2\phi)+1-b]$, and algorithm	x	x

The meaning of used symbols in the table:
For the used modeling approach; S: Statistical, G: Geometrical, E: Empirical, IG: Integral Geometry. The building's height distribution; Ryl: Rayleigh, $\mathcal{U}$: uniform. The communication channel types; G2G: ground-to-ground or terrestrial, G2A: ground-to-air, A2G: air-to-ground, and S2G: satellite-to-ground. The models variables $d_{2D}, h, \theta, \phi, w_b, w_s, f_c$ are ground distance, altitude difference ($h = h_{tx} - h_{rx}$), elevation angle, azimuth angle, width of building, width of street, and center frequency of the communication channel, respectively. The function $G(\cdot)$ is the complementary cumulative distribution function (CCDF) of the log-normal distribution. $Q(\cdot)$ is the Q-function. $erf(\cdot)$ is the error function. The symbols a, b, c, d, and e can be a single variable, single curve-fitting factor, or a simple mathematical function on more than one variable. For further details refer to the original reference.

Moreover, the 1D class of the LoS probability models is introduced in [13], [17], [24], [16], [14], [12], [20], and [21] as well. [13] optimized the altitude for low-altitude platforms for public safety to maximize coverage in remote areas and provides a LoS probability model, which is expressed as a curve-fitting of the sigmoid function. The model is dependent on elevation angle; however, it does not present how to represent the fitting parameters with ITU-R layout parameters, which makes it hard to generalize the model even though it is one of the most referenced models.

[24] investigates the behavior of large-scale fading in urban layouts that follows the ITU-R model and proposes an approximate LoS probability model as an exponential function of Q-function that is dependent on the receiver's height, elevation angle, and ITU-R layout parameters. The study simulates three-dimensional ray-tracing using wireless in-site software for an air-to-air (A2A) communication channel. Although the buildings are distributed as a two-dimensional HPPP, the model in [24] follows the 1D class. The models [11] and [37] are proposed for satellite-to-ground (S2G) communication, while the second uses the continuous-space Markov chain and algorithms to characterize the LoS status.

The two-dimensional derivation of the LoS probability model replaces the direct ray connecting between the transmitter and the receiver with some area and calculates the probability of no building in that area. For example, the study in [23] used the random shape theory to model the LoS probability based on the random shapes of buildings, particularly the dimensions of the building's width and length. In [26], circles with radius r are as-

sumed about the location of transmitter and receiver and calculate the probability of having zero buildings within the area or a rectangular shape with width equals $2r$ and length equals d_{2D}. The circle radius is assumed to be the radius of a cylindrical building. [23] does not validate the model against real-world nor ITU-R urban layout configuration parameters, while the work in [26] provides an alignment method to convert the ITU-R parameters or real-world measurements into the terms of its proposed model in addition to the alignment equation to adapt the heights of real-world buildings to be used with the proposed model, which is based on the log-normal distribution.

In addition, the work [29] presents a geometric-based LoS probability model for ground-to-air (G2A) communication channels for the 5G mm-wave frequency. The proposed model is modeled in a 2D MPLP layout for a special case, which is when the ground base stations are located on crossroads. The model is composed of nested exponential and error functions in the x- and y-directions of the layout coordinates. The complexity of the model and its incompatibility with the ITU-R make it hard to generalize. The study [22] provides a statistical LoS probability model based on the ground distance from the receiver to the first building along the connecting ray between the transmitter and the receiver for the A2G channel. Unlike most of the studies that follow a curve-fitting approach, the model provides the fitting parameters as functions of street and building widths, which can be calculated from the ITU-R layout model. Although the study derived two formulas for the LoS probability, we chose to present the general one as expressed in table 3. However, [22] validates the model with ground distance only, while altitude difference is input to the exponential- and error-function terms of the model, which could impact the performance for high-altitude placement of UAVs. [35] proposed a LoS probability model for the special case where the receiver is mounted on the rooftop of buildings.

The three-dimensional modeling approach considers the absence of buildings within a volume between the transmitter and receiver. The volume of the LoS zone can be the intersection of the 2D horizontal plane and the Fresnel zone, as in [25] or simply by considering the volume of the ellipse of the Fresnel zone. In [25], the model is derived using stochastic geometry approach assumptions of the intersection between the two-dimensional homogeneous Poisson Point Process and the Fresnel clearance zone. Although the introduced model is frequency-dependent, the wavelength term is neutralized in this model for high frequencies, and it is simplified with the expected width $\mathbb{E}_W$ and length $\mathbb{E}_L$ of buildings that are set to a fixed value equal to 15 [m]. Other parameters are set as follows: $\beta = \frac{0.1}{\mathbb{E}_W \mathbb{E}_L}$, $h_{tx} = 35$ [m], $h_{rx} = 1.5$ [m], and the range building lower and upper heights ($h_{b,lo} = 10$ [m], $h_{b,up} = 100$ [m]). A similar approach is introduced in [18] by calculating the LoS probability for the intersection of building geometry with both the clearance zone and the ellipse of the 3D shape of the Fresnel zone.

The study in [19] modifies the ITU-R LoS probability model by considering the Fresnel zone to provide a three-dimensional line-of-sight probability model. Based on the proposed stochastic analytical model, it develops a machine learning model that uses a back propagation neural network (BPNN) to approximate and simplify the LoS probability. The study validates the proposed model with a ray-tracing simulation using the Monte-Carlo method. In [30], the authors considered that the energy of the signal propagation path is distributed within the entire Fresnel zone and modified the ITU-R model to meet the first-order Fresnel zone for the A2G channel. Another 3D geometry-based LoS probability model is introduced in [31], which investigates the impact of buildings' shadows on nearby streets. The study assumed three examples of a building's height. The first is when a building has a maximum height of $h_{i,max}$ and can block the sight of all the streets behind it from a transmitter (i.e., a UAV or airborne base station). In the case that the street is partially seen, that implies there exists an i-th building with a maximum height $h_{i,lo}$ lower than the line-of-sight ray that allows the LoS status or with a maximum height $h_{i,up}$ greater than the line-of-sight ray that blocks the sight, resulting in a NLoS condition. The model is expressed with a difference of two error functions, as shown in table 3; however, The model cannot stand alone because it depends on the relative azimuth direction of the UAV to the grid of buildings. Thus, the authors proposed an algorithm to calculate the LoS probability for different conditions.

The line-of-sight probability is also modeled with other aspects than the ITU-R urban layout model, such as the 3GPP (The 3rd Generation Partnership Project), which presented distance-dependent models for urban micro (UMa) and micro (UMi) cell implementations for different ranges of frequencies as in 3GPP TR 38.900 [36] and 3GPP TR 38.901 [38], curve-fitting with specific functions, and machine learning. Similar models to the standard 3GPP are introduced in [17], [14]. The LoS probability models of the 3GPP are formulated by considering the transmitter and receiver's heights to determine the distance break-point d_{Bp} for UMa and UMi. If the distance between transmitter and receiver is less than the break-point distance, the LoS probability equals one. If not, we calculate the LoS probability using various inputs like the distance between the transmitter and receiver, transmitter heights, center frequency, and the cell deployment scenario. For example, the reader may refer to table 7.4.2-1 in [36] or table 7.4.2-1 in [38] for more details. However, the 3GPP model is suitable for short distances, where the break-point d_{Bp} distance defines the range of LoS status for shorter distances than the break-point, which is tuned to 18 meters for the UMi scenario [36],

[17].

The work in [14] proposed another modification to the 3GPP model. The authors introduced a K-nearest neighbors (KNN)-based strategy to classify LoS and NLoS, then developed a two-layer back propagation neural network (BPNN)-based parameter estimation method to find the relationship between model parameters and the altitude of the UAV. The proposed model is tested against ray-tracing data. The work in [40] optimizes the throughput of ground UE in hot-spot areas by adopting an airborne base station. The LoS probability model of the proposed A2G channel is modeled using elevation angle θ [radian] dependent expression with two fitting parameters of the sigmoid function (also known as S-curve), similar to [13] with fixed fitting parameters for a and b to 9.61 and 0.16, respectively. The LoS probability model is used within a multi-agent environment deep deterministic policy gradient (MADDPG) algorithm, which is an extension of the DDPG.

The curve-fitting models are presented in [10], [13], [12], [20], [21], and [22]. The study in [10] looked at mobile communications from high-altitude platforms (HAPs) in four different urban settings. They used five empirical curve fitting parameters to model the LoS probability. The study in [12] uses the two-ray propagation model and the knife edge diffraction model to analytically and numerically demonstrate the validity of defining the LoS condition based on the intrusion ratio of an obstruction in the first Fresnel zone. It formulates a deterministic mathematical model based on two-ray propagation to determine the exact LoS within the ellipsoid of the first Fresnel zone. The focal points of the ellipse are situated at the transmitter and receiver locations, with the fixed height of the transmitter at 300 m. The stretched exponential function (also known as the complementary cumulative distribution function of the Weibull distribution) is used to simulate the LoS probability. Only the study in [22] provides the fitting parameter as a function of street and building widths, so it is possible to translate the ITU-R layout configuration parameters into the fitting. This type of translation is important for generalizing the model because it allows it to be applicable to various layout parameters.

4. EMPIRICAL VALIDATION

As we discussed in the previous section about generalizing existing models, this section aims to validate the generality of excising LoS probability models in the current literature by comparing their performance to the results of a ray-tracing simulation. Unfortunately, we did not find an open-source tool that could simulate synthetic urban layouts following the ITU-R urban configuration parameters, adding that previous studies used property software like MATLAB to implement the ray-tracing simulation. Simulating ray-tracing between points in a 3D space using ordinary simulation methods is difficult because it requires extensive object implementation and a thorough understanding of each object's transformation, including location, orientation, scale, and relative calculation.

Game engines enhance the performance of computing and visualizing 3D graphics on regular personal computers at a reasonable cost. Additionally, they offer features such as collision detection, transformations, mobility, physics systems, networking, and artificial intelligence. These capabilities can be used in accurate research for 5G networks and beyond. Therefore, we developed an open-source game-engine-based framework that takes advantage of the significant advancements in game-engine technologies, which have enabled the possibility of running 3D environments on personal computers.

We simulated the ray-tracing for the four urban configurations in table 2 using the setup in table 4, where the four-element tuples in the simulation setup parameters are for high-rise urban, dense urban, urban, and suburban, respectively.

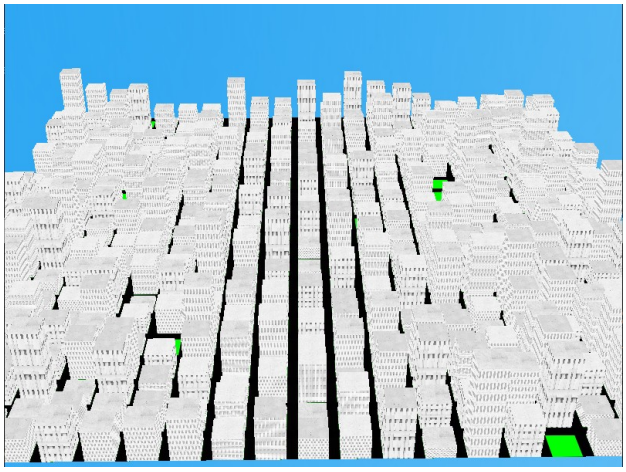

Figure 3. High-rise Urban, 3D synthetic layout as generated by Panda5gSim.

We randomly generate the position of buildings to provide a total number equal to $|R|\beta$, where $|R|$ is the area measure of the simulation region and measures in square kilometers. We generate the height of the buildings using the Rayleigh distribution. For example, the generated 3D synthetically urban layouts for the standard environment configurations in Table 2 are shown in the Figures 3 to reffig:Suburban. The Figures 3, 4, 5, and 6 represent high-rise urban, dense urban, urban, and suburban, respectively.

Figure 7 presents a three-dimensional surface plot for the ray-tracing probability, which we extract as a function in the direction of ground distance, denoted by d_{2D}, and altitude difference between UAV and ground user, denoted by $h_{tx} - h_{rx}$. The figure depicts four urban con-

Table 4. Simulation setup parameters.

Parameter	Distribution	Unit	Values
Simulation area	-	km^2	(1.2×1.2)
Number of buildings	Grid	-	(432, 432, 720, 1080)
Number of UAVs	Uniform	-	25
Number of users	Uniform	-	(1024, 1024, 1771, 2211)
Height of UAVs	Uniform	meter	U(51.5, 1001.5, 50)
Height of UEs	Fixed	meter	1.5

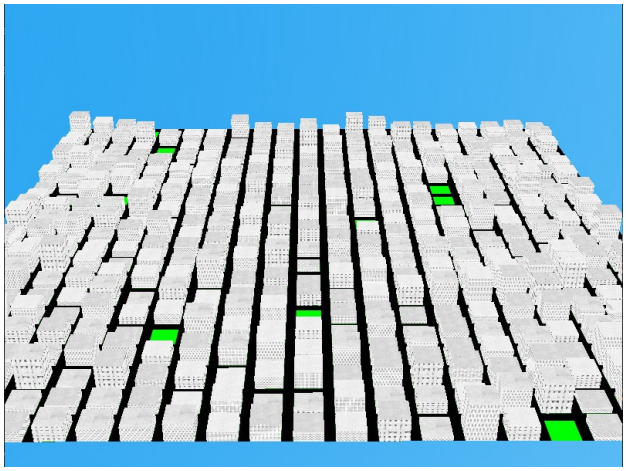

Figure 4. Dense Urban, 3D synthetic layout as generated by Panda5gSim.

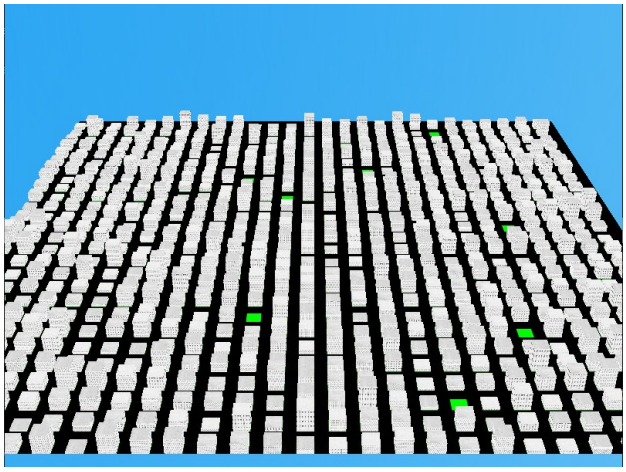

Figure 5. Urban, 3D synthetic layout as generated by Panda5gSim.

figurations, which are, from left to right, high-rise urban, dense urban, urban, and suburban. We observe that the altitude difference more significantly affects the ray-tracing LoS status than the ground distance. The four sub-figures in Figure 7 describe the ray-tracing LoS probability P_{LoS} that varies by color from zero to one. The zero is the blue color, while the one is the red color.

Figure 7 shows that the distance has a significant impact in high-rise urban, where the shadow of buildings is greater than other urban layouts. In the suburban sub-figure, the P_{LoS} reaches the one faster than other sub-figures. That indicates a proportional relation between P_{LoS} in the altitude direction and the width of the streets.

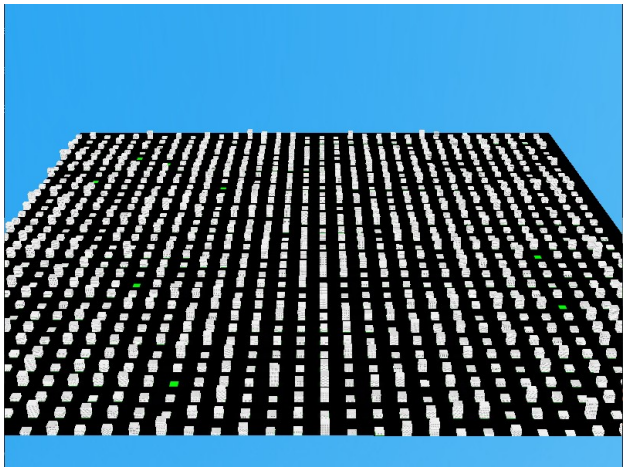

Figure 6. Suburban, 3D synthetic layout as generated by Panda5gSim.

In general, we can see that the P_{LoS} can be modeled as a bivariate probability of two marginal functions expressed in terms of exponential and error functions. The concavity in the suburban sub-figure is because we used the cubic polynomial function to smooth the surface of the P_{LoS}. Keep in mind that the higher the altitude, the higher P_{LoS}.

Moreover, we chose to compare the A2G LoS probability models to illustrate the impact of various functions used in different models. We compared the following models: [9], [24], [16], [26], [30], [22], [31]. It is known that the model [9] is used in the G2G communication channels, but we included it in the comparison to show the difference between its performance and the ray-tracing, especially since recent models such as [30] followed it.

Figure 8 compares the performance of the LoS probability models compared to ray-tracing according to the ground distance between UAVs and ground users. The decay of the ray-tracing LoS is faster in high-rise and gradually gets slower as the γ decreases. By comparing to the G2G models as in [9], we observe that the decay of the ray-tracing is less in the A2G case. Because both follow the same formula, the curve of [30] is almost identical to [9]. Although [24] uses the Q-function, which is similar to the complementary of the error function in [22], both have similar curves. That is because the first building assumption in [22] reduces the effect of the long ground distance. However, the Q-function term produces a near-zero response for the height of ground users, which, in consequence, elevates the decay of the exponential part

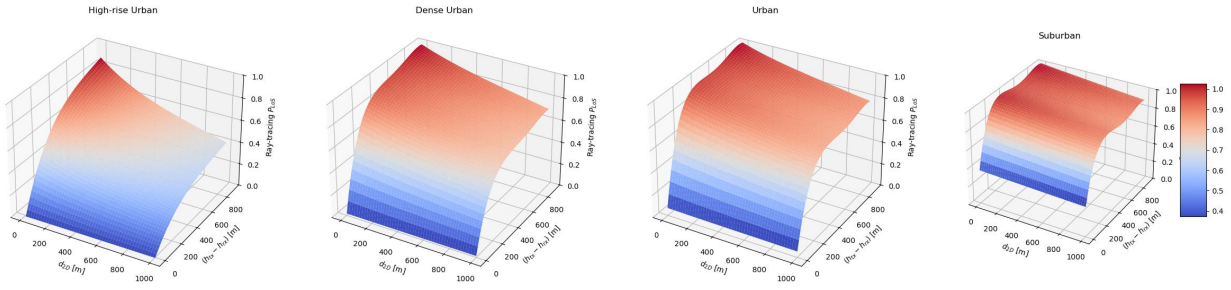

Figure 7. A three-dimensional representation of ray-tracing LoS probability.

of the model. Similarly, the CCDF and the error-function parts do for the models [26] and [31].

Figure 9 depicts the relationship between ray-tracing LoS probability and altitude differences. The results of LoS models show that the LoS probability in most of the curves increases with altitude. However, the models under comparison do not accurately predict the LoS status. The curve of [31] is almost horizontal because it depends on an algorithm that is not within the scope of these evaluation objectives. Again, we observe that [24] and [22] have limited applicability in the A2G communication channel because the effect of ground distance and altitude difference on the LoS probability needs further tuning.

From Figure 8 and Figure 9, we observed that the LoS models, expressed in terms of distance, altitude, and ITU-R urban configuration parameters, trend with the ray-tracing in both figures, but they lack accuracy. These models are [9, 16, 30]. In contrast, the model [26] has almost a horizontal curve in the ground distance direction because it was not developed for the ITU environment. The model [22] is well-formulated, but its results in a general environment are not stable because it uses a curve fitting parameter that cannot be generalized. The result of [31] shows that the model cannot stand alone without its algorithm. Regardless of its low performance, the model [16] has a better trend with the curve of the ray-tracing, so it is a good candidate for future enhancement.

The result in Figure 8 and Figure 9 is unexpectedly show that some old models, such [16] and [26], have better performance in the standard urban environment if we variate the ground distance and the altitude difference from 0 to 1000 meter. For example, the best performance in high-rise urban is scored by [16] with root mean square error (RMSE) equals 0.29. The model [26] scored the best RMSE in dense urban, urban and suburban with 0.19, 0.18, and 0.06, respectively. Both [16] and [26] are modeled using exponential and error functions. Note that the Log-Normal function in [26] can be expressed using error function. The mathematical equation of [16] is expressed in (19), while the model [26] is expressed in (20); where r_0 is the radius of cylinder buildings and $G(h_i) = 1 - F(h_i)$ is the CCDF of the log-normal distribution that is given in (13) while h_i is given in (11).

Our experiments reveal a small exponential decay in the LoS probability, while the altitude axis significantly influences it, unlike the G2G LoS probability, which follows an exponential function on the ground distance axis. We investigated the correlation between the LoS toward ground distance and toward altitude differences and found low correlation coefficients, with the highest being about 0.1 for high-rise urban. This means the possibility of modeling the two-dimensional LoS probability model using a product of two distinct functions.

We implement the proposed ray-tracing simulation method, where the generation of the 3D urban layout is conducted with computer vision techniques using Python programming language and some scientific libraries, such as NumPy, SciPy, openCV [41] while the 3D environment and the ray-tracing are developed using Panda3 [42] game engines. Part of the 5G communication channel in our implementation follows the open-source work presented in [43]. We developed an open-source implementation of the proposed ray-tracing simulation approach and named it **Panda5gSim**. The code, generated datasets, and performance evaluation results can be found on GitHub [8].

5. CHALLENGES AND OPEN OPPORTUNITIES

Based on the reviews and the empirical validation in previous section, this section highlights the challenges to the LoS probability modeling and suggests some research opportunities.

- **The complexity of modeling urban environments**: Usually, we model the LoS probability for urban environments. Existing works model the urban environments using stochastic geometry, stochastic processes, and real-world datasets. The stochastic geometry approach can provide general models, but it relies on specific arrangements of objects in the 3D

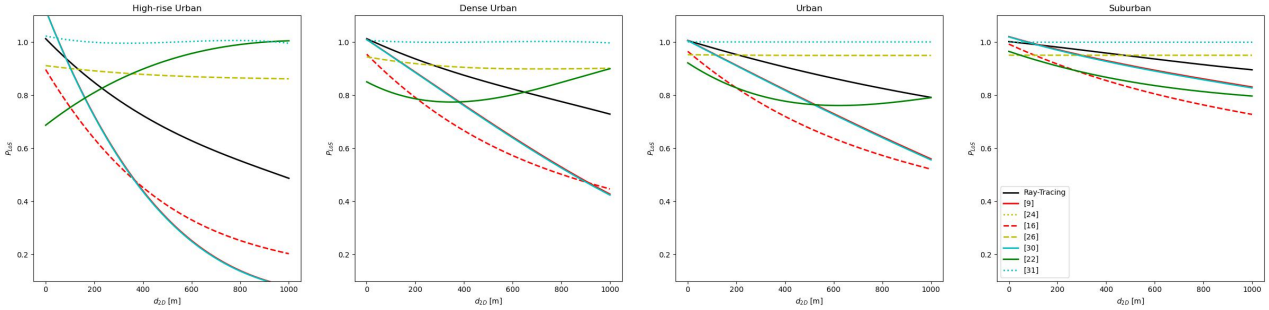

Figure 8. The performance of LoS probability models compared to ray-tracing in terms of ground distance difference between UAV and ground user.

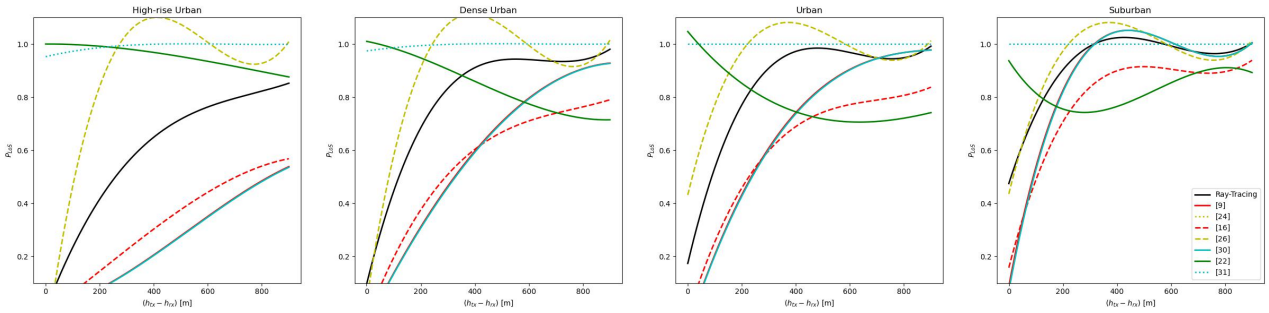

Figure 9. The performance of LoS probability models compared to ray-tracing in terms of Altitude difference between UAV and ground user.

space. The statistical models that rely on real-world data are known to be more accurate, but that accuracy has its cost. Real-world data requires a lot of time to collect measurements and is not cost-efficient. Ray-tracing simulation is a reasonable alternative to real-world data; however, it has a high computational cost [44]. Reducing the complexity of ray-tracing simulation in 3D synthetic urban layouts is a challenging task, especially for low-budget researchers. We contribute to this with our Panda5gSim, but it still needs further enhancement. For future research, we encourage game engine-based simulation to utilize their capabilities in 3D modeling and straight-forward calculation for transformations and ray-tracing.

- **The Directional LoS probability models**: The case of using omnidirectional antennas on UAVs or GUTs dominates current literature on the LoS probability models. Using omnidirectional antennas in urban environments can increase the interference in the wireless network because the flying altitude of the UAV can be in line-of-sight with a large number of users and base stations. Although directional antennas are known to solve this problem, current LoS probability models do not account for the directional scenario. Modeling LoS probability for directional antennas is valid future research.
- **The Mobility**: The mobility of both the UAV and the gUT is not taken into account by existing LoS models. Even though we determine the LoS condition from point to point, mobility affects the duration of being in LoS. Mobility-aware LoS probability studies can contribute to the contact time, also known as sojourn time. There is still an opportunity to model sojourn time using ray-tracing simulation and similar approaches used in LoS probability.
- **Multivariate probability**: As shown in Table 3, many studies used (d_{2D}, h) as model input. Existing models are formed through univariate analysis. Higher order of analysis can be a future work to formulate the LoS probability using bivariate or multivariate probability.

$$P_1(d_{2D}, h_{tx}, h_{rx}) = exp\left(-\sqrt{\frac{\alpha\beta\pi}{2}} \cdot \frac{\gamma d_{2D}}{(h_{tx} - h_{rx})} \cdot erf\left(\frac{(h_{tx} - h_{rx})}{\sqrt{2\gamma}}\right)\right), \tag{19}$$

$$P_2(d_{2D}, h_{tx}, h_{rx}) = exp\left(-2r_0\beta(d_{2D} - \frac{\pi}{2}r_0)G(h_i)\right) \tag{20}$$

Following our findings in the previous section, we propose studying the LoS probability as a bivariate probability with exponential and log-normal marginal functions.

6. CONCLUSION

Suspendisse vel felis. Ut lorem lorem, interdum eu, tincidunt sit amet, laoreet vitae, arcu. Aenean faucibus pede eu ante. Praesent enim elit, rutrum at, molestie non, nonummy vel, nisl. Ut lectus eros, malesuada sit amet, fermentum eu, sodales cursus, magna. Donec eu purus. Quisque vehicula, urna sed ultricies auctor, pede lorem egestas dui, et convallis elit erat sed nulla. Donec luctus. Curabitur et nunc. Aliquam dolor odio, commodo pretium, ultricies non, pharetra in, velit. Integer arcu est, nonummy in, fermentum faucibus, egestas vel, odio.

7. CONCLUSION

Current literature presents the LoS probability models for several communication channels, but it lacks a comprehensive review that compares and summarizes those models. In this paper, we reviewed the LoS probability models, focusing on the modeling approaches and the mathematical forms. We elaborately describe different parts of the modeling approaches that contribute to the final models. For instance, we present the mathematical representations of building and street geometries, as well as the distribution process, in addition to the abstract mathematical structures of the LoS probability models. This paper concentrates on large stationary blockages. We discovered that, due to the complexity of modeling a large number of 3D layouts, most existing models have focused on a few urban layouts. We developed a 3D synthetic urban layout generator that is based on game engine technology to simulate any ITU-R P.1410 urban layouts and collect the ray-tracing for the A2G scenario. We validated the proposed game engine-based simulation and compared the performance of some existing LoS models to the ray-tracing. The game engine simulation shows decent capabilities that deserve further improvements. Finally, we addressed some of the biggest challenges and gaps in the current LoS probability literature and suggested some valid opportunities.

REFERENCES

[1] Giovanni Geraci et al. “What Will the Future of UAV Cellular Communications Be? A Flight From 5G to 6G”. In: *IEEE Commun. Surv. & Tutorials* 24.3 (2022), pp. 1304–1335. ISSN: 1553-877X. DOI: 10.1109/COMST.2022.3171135.

[2] “A Comprehensive Review for Typical Applications Based Upon Unmanned Aerial Vehicle Platform”. In: *IEEE J. Sel. Top. Appl. Earth Obs. Remote. Sens.* 15 (2022), pp. 9654–9666. ISSN: 2151-1535. DOI: 10.1109/JSTARS.2022.3216564.

[3] Nan Cheng et al. “AI for UAV-Assisted IoT Applications: A Comprehensive Review”. In: *IEEE Internet Things J.* 10.16 (Aug. 2023), pp. 14438–14461. ISSN: 2327-4662. DOI: 10.1109/JIOT.2023.3268316.

[4] George R MacCartney et al. “Millimeter-Wave Human Blockage at 73 GHz with a Simple Double Knife-Edge Diffraction Model and Extension for Directional Antennas”. In: *2016 IEEE 84th Vehicular Technology Conference (VTC-Fall)*. 2016, pp. 1–6. DOI: 10.1109/VTCFall.2016.7881087.

[5] Richard J Weiler et al. “Environment Induced Shadowing of Urban Millimeter-Wave Access Links”. In: *IEEE Wirel. Commun. Lett.* 5.4 (Aug. 2016), pp. 440–443. ISSN: 2162-2345. DOI: 10.1109/LWC.2016.2581820.

[6] Dmitri Moltchanov et al. “A Tutorial on Mathematical Modeling of 5G/6G Millimeter Wave and Terahertz Cellular Systems”. In: *IEEE Commun. Surv. & Tutorials* 24.2 (2022), pp. 1072–1116. ISSN: 1553-877X. DOI: 10.1109/COMST.2022.3156207. URL: https://ieeexplore.ieee.org/abstract/document/9726709.

[7] Nadezhda Chukhno et al. “Models, Methods, and Solutions for Multicasting in 5G/6G mmWave and sub-THz Systems”. In: *IEEE Commun. Surv. & Tutorials* (2023), p. 1. ISSN: 1553-877X. DOI: 10.1109/COMST.2023.3319354. URL: https://ieeexplore.ieee.org/abstract/document/10263616.

[8] Basheer Raddwan and Ibrahim A Al-Baltah. *Panda5gSim*. 2024. URL: https://github.com/yemenlinux/panda5gsim.

[9] ITU-R. *Propagation Data and Prediction Methods Required for the Design of Terrestrial Broadband Radio Access Systems in a Frequency Range from 3 to 60 GHz*. Tech. rep. 2012. URL: https://www.itu.int/dms%7B%5C_%7Dpubrec/itu-r/rec/p/R-REC-P.1410-5-201202-I!!PDF-E.pdf.

[10] Jaroslav Holis and Pavel Pechac. “Elevation Dependent Shadowing Model for Mobile Communications via High Altitude Platforms in Built-Up Areas”. In: *IEEE Trans. on Antennas Propag.* 56.4 (Apr. 2008), pp. 1078–1084. ISSN: 1558-2221. DOI: 10.1109/TAP.2008.919209.

[11] Akram Al-Hourani and Ismail Guvenc. “On Modeling Satellite-to-Ground Path-Loss in Urban Environments”. In: *IEEE Commun. Lett.* 25.3 (Mar. 2021), pp. 696–700. ISSN: 1558-2558. DOI: 10.1109/LCOMM.2020.3037351.

[12] Yassine Hmamouche, Mustapha Benjillali, and Samir Saoudi. “Fresnel Line-of-Sight Probability With Applications in Airborne Platform-Assisted Communications”. In: *IEEE Trans. on Veh. Technol.* 71.5 (May 2022), pp. 5060–5072. ISSN: 1939-9359. DOI: 10.1109/TVT.2022.3151461.

[13] Akram Al-Hourani, Sithamparanathan Kandeepan, and Simon Lardner. “Optimal LAP Altitude for Maximum Coverage”. In: *IEEE Wirel. Commun. Lett.* 3.6 (Dec. 2014), pp. 569–572. ISSN: 2162-2345. DOI: 10.1109/LWC.2014.2342736.

[14] Minghui Pang et al. “Machine learning based altitude-dependent empirical LoS probability model for air-to-ground communications”. In: *Front. Inf. Technol. & Electron. Eng.* 23.9 (2022), pp. 1378–1389. ISSN: 2095-9230. DOI: 10.1631/FITEE.2200041. URL: https://doi.org/10.1631/FITEE.2200041.

[15] Mohammad Taghi Dabiri and Mazen Hasna. “3D Uplink Channel Modeling of UAV-Based mmWave Fronthaul Links for Future Small Cell Networks”. In: *IEEE Trans. on Veh. Technol.* 72.2 (Feb. 2023), pp. 1400–1413. ISSN: 1939-9359. DOI: 10.1109/TVT.2022.3209988.

[16] Honggu Kang et al. “Secrecy-Aware Altitude Optimization for Quasi-Static UAV Base Station Without Eavesdropper Location Information”. In: 23.5 (May 2019), pp. 851–854. ISSN: 1558-2558. DOI: 10.1109/LCOMM.2019.2909880.

[17] Italo Atzeni, Jesús Arnau, and Marios Kountouris. "Downlink Cellular Network Analysis With LOS/NLOS Propagation and Elevated Base Stations". In: *IEEE Trans. on Wirel. Commun.* 17.1 (Jan. 2018), pp. 142–156. ISSN: 1558-2248. DOI: 10.1109/TWC.2017.2763136.

[18] Zhuangzhuang Cui et al. "Frequency-Dependent Line-of-Sight Probability Modeling in Built-Up Environments". In: *IEEE Internet Things J.* 7.1 (Jan. 2020), pp. 699–709. ISSN: 2327-4662. DOI: 10.1109/JIOT.2019.2947782.

[19] "Geometry-Based Stochastic Line-of-Sight Probability Model for A2G Channels Under Urban Scenarios". In: *IEEE Trans. on Antennas Propag.* 70.7 (July 2022), pp. 5784–5794. ISSN: 1558-2221. DOI: 10.1109/TAP.2022.3161277.

[20] Mengan Song et al. "Air-to-Ground Large-Scale Channel Characterization by Ray Tracing". In: *IEEE Access* 10 (2022), pp. 125930–125941. ISSN: 2169-3536. DOI: 10.1109/ACCESS.2022.3224776.

[21] Mengan Song et al. "Line-of-sight probability for UAV communications in 3D grid urban streets". In: *Electron. Lett.* 59.20 (2023), e12979. DOI: https://doi.org/10.1049/ell2.12979. URL: https://ietresearch.onlinelibrary.wiley.com/doi/abs/10.1049/ell2.12979.

[22] Imran Mohammed et al. "Closed Form Approximations for UAV Line-of-Sight Probability in Urban Environments". In: *IEEE Access* 11 (2023), pp. 40162–40174. DOI: 10.1109/ACCESS.2023.3267808.

[23] Tianyang Bai, Rahul Vaze, and Robert W Heath. "Analysis of Blockage Effects on Urban Cellular Networks". In: *IEEE Trans. on Wirel. Commun.* 13.9 (2014), pp. 5070–5083. ISSN: 1558-2248. DOI: 10.1109/TWC.2014.2331971.

[24] Lai Zhou et al. "Propagation Characteristics of Air-to-Air Channels in Urban Environments". In: *2018 IEEE Global Communications Conference (GLOBECOM)*. Dec. 2018, pp. 1–6. DOI: 10.1109/GLOCOM.2018.8647360.

[25] "Analysis of Frequency-Dependent Line-of-Sight Probability in 3-D Environment". In: *IEEE Commun. Lett.* 22.8 (Aug. 2018), pp. 1732–1735. ISSN: 1558-2558. DOI: 10.1109/LCOMM.2018.2842763.

[26] Akram Al-Hourani. "On the Probability of Line-of-Sight in Urban Environments". In: *IEEE Wirel. Commun. Lett.* 9.8 (Aug. 2020), pp. 1178–1181. ISSN: 2162-2345. DOI: 10.1109/LWC.2020.2984497.

[27] François Baccelli and Xinchen Zhang. "A correlated shadowing model for urban wireless networks". In: *2015 IEEE Conference on Computer Communications (INFOCOM)*. Apr. 2015, pp. 801–809. DOI: 10.1109/INFOCOM.2015.7218450.

[28] Enass Hriba, Matthew C Valenti, and Robert W Heath. "Optimization of a Millimeter-Wave UAV-to-Ground Network in Urban Deployments". In: *MILCOM 2021 - 2021 IEEE Military Communications Conference (MILCOM)*. Nov. 2021, pp. 861–867. DOI: 10.1109/MILCOM52596.2021.9653132.

[31] Abdul Saboor et al. "A Geometry-Based Modelling Approach for the Line-of-Sight Probability in UAV Communications". In: *IEEE Open J. Commun. Soc.* 5 (2024), pp. 364–378. ISSN: 2644-125X. DOI: 10.1109/OJCOMS.2023.3341627.

[32] City of Melbourne - Open Data Portal. *No Title*. URL: https://data.melbourne.vic.gov.au/.

[29] Margarita Gapeyenko et al. "Line-of-Sight Probability for mmWave-Based UAV Communications in 3D Urban Grid Deployments". In: *IEEE Trans. on Wirel. Commun.* 20.10 (Oct. 2021), pp. 6566–6579. ISSN: 1558-2248. DOI: 10.1109/TWC.2021.3075099.

[30] Minghui Pang et al. "Geometry-Based Stochastic Probability Models for the LoS and NLoS Paths of A2G Channels Under Urban Scenarios". In: *IEEE Internet Things J.* 10.3 (Feb. 2023), pp. 2360–2372. ISSN: 2327-4662. DOI: 10.1109/JIOT.2022.3211524.

[33] New York City—Open Data Portal. *No Title*. URL: https://opendata.cityofnewyork.us/data/.

[34] Akram Al-Hourani, Sithamparanathan Kandeepan, and Abbas Jamalipour. "Modeling air-to-ground path loss for low altitude platforms in urban environments". In: *2014 IEEE Global Communications Conference*. Dec. 2014, pp. 2898–2904. DOI: 10.1109/GLOCOM.2014.7037248.

[35] "Closed-Form UAV LoS Blockage Probability in Mixed Ground- and Rooftop-Mounted Urban mmWave NR Deployments". In: *Sensors* 22.3 (2022). ISSN: 1424-8220. DOI: 10.3390/s22030977. URL: https://www.mdpi.com/1424-8220/22/3/977.

[36] 3GPP TR 38.900 - V14.2.0. *Study on channel model for frequency spectrum above 6 GHz*. Tech. rep. 2017. URL: https://portal.etsi.org/TB/ETSIDeliverableStatus.aspx.

[37] Akram Al-Hourani. "Line-of-Sight Probability and Holding Distance in Non-Terrestrial Networks". In: *IEEE Commun. Lett.* 28.3 (Mar. 2024), pp. 622–626. ISSN: 1558-2558. DOI: 10.1109/LCOMM.2024.3357285.

[38] 3GPP TR 38.901 V16.1.0. *Study on channel model for frequencies from 0.5 to 100 GHz*. Tech. rep. 2020. URL: http://www.etsi.org/standards-search.

[39] Pekka Kyösti et al. *IST-4-027756 WINNER II D1. 1.2 V1. 2 WINNER II Channel Models*. Tech. rep. 82. 2007, pp. 39–92. DOI: 10.1002/9780470748077.ch3.

[40] Yikun Zhao et al. "MADRL-Based 3D Deployment and User Association of Cooperative mmWave Aerial Base Stations for Capacity Enhancement". In: *Chin. J. Electron.* 32.2 (Mar. 2023), pp. 283–294. ISSN: 2075-5597. DOI: 10.23919/cje.2021.00.327.

[41] OpenCV. *Open Source Computer Vision Library*. URL: https://github.com/opencv/opencv (visited on 2024).

[42] Panda3D. *Panda3D*. URL: https://github.com/panda3d/panda3d (visited on 2024).

[43] Edward J Oughton et al. "An Open-Source Techno-Economic Assessment Framework for 5G Deployment". In: *IEEE Access* 7 (2019), pp. 155930–155940. ISSN: 2169-3536. DOI: 10.1109/ACCESS.2019.2949460.

[44] Mattia Lecci et al. "Accuracy Versus Complexity for mmWave Ray-Tracing: A Full Stack Perspective". In: *IEEE Trans. on Wirel. Commun.* 20.12 (Dec. 2021), pp. 7826–7841. ISSN: 1558-2248. DOI: 10.1109/TWC.2021.3088349.